

ADP-02-99/T537, LTH564

QUENCHED CHIRAL PHYSICS IN BARYON MASSES

R. D. YOUNG, D. B. LEINWEBER AND A. W. THOMAS

Special Research Centre for the Subatomic Structure of Matter, and Department of Physics and Mathematical Physics, University of Adelaide, Adelaide SA 5005, Australia
E-mail: ryoung@physics.adelaide.edu.au; dleinweb@physics.adelaide.edu.au;
athomas@physics.adelaide.edu.au

S. V. WRIGHT

*Division of Theoretical Physics, Department of Mathematical Sciences,
 University of Liverpool, Liverpool L69 3BX, U.K.
 E-mail: svwright@amtp.liv.ac.uk*

Recent work has identified that the primary differences between quenched and dynamical spectroscopy can be described by chiral loop effects. Here we highlight the features of this study.

1. Introduction

Chiral symmetry has long been known to play an important role in the low energy properties of QCD. Theoretical studies of the non-perturbative features of QCD, expressed in terms of the fundamental theory, have proven to be most successful in the field of lattice gauge theory. Lattice studies are typically restricted to relatively large values of the u and d masses, where chiral effects are highly suppressed. As a consequence, direct observation of chiral properties is a challenge in lattice simulations. The study of low-lying baryon spectroscopy in both quenched and full QCD has provided a direct connection between lattice results and chiral physics^{1,2}.

The fact that one is restricted to quark masses much larger than the physical values means that, in addition to all the usual extrapolations (e.g. to the infinite volume and continuum limits), if one wants to compare with empirical hadron observables, one must also have a reliable method of extrapolation to the chiral limit. Any such extrapolation must incorporate the appropriate chiral corrections, arising from Goldstone boson loops, which give rise to rapid, non-linear variations as the chiral limit is approached. The importance of incorporating such behaviour has been successfully demonstrated for a number of hadronic observables, see Ref. [3] for a review and the references contained

therein.

The quenched approximation is a widely used tool for studying non-perturbative QCD within numerical simulations of lattice gauge theory. With an appropriate choice of the lattice scale and at moderate to heavy quark masses, this approximation has been shown to give only small, systematic deviations from the results of full QCD with dynamical fermions. Although no formal connection has been established between full and quenched QCD, the similarity of the results has led to the belief that the effects of quenching are small and hence that quenched QCD provides a reasonable approximation to the full theory⁴. Under a more reliable choice of lattice scale, where chiral effects are negligible, clear differences are observed between quenched and dynamical results⁵.

2. Chiral Physics and the Quenched Approximation

Chiral symmetry is spontaneously broken in the ground state of QCD. As a consequence, the pion is a Goldstone boson characteristic of this broken symmetry. The pion mass then behaves as $m_\pi^2 \propto m_q$, the well known Gell-Mann–Oakes–Renner (GOR) relation. In principle, this relation is only guaranteed for quark masses near zero. Explicit lattice calculations show that it holds over an enormous range, as high as $m_\pi \sim 1$ GeV. These almost massless Goldstone bosons couple strongly to low-lying baryon states — particularly the nucleon (N) and delta (Δ).

Meson-loop diagrams involving Goldstone bosons coupling to baryons give rise to non-analytic behaviour of baryon properties as a function of quark mass. At light quark masses these corrections are large and rapidly varying. At heavy quark masses these contributions are suppressed and hadron properties are smooth, slowly varying functions of quark mass. The scale of this transition is characterised by the inverse size of the pion-cloud source. Below pion masses of about 400–500 MeV these non-analytic contributions become increasingly important, while they rapidly become negligible above this point. Since lattice simulations are typically restricted to the domain where $m_\pi \gtrsim 500$ MeV, these rapid-varying chiral effects must be incorporated phenomenologically.

Within the quenched approximation dynamical sea quarks are absent from the simulation. As a consequence the structure of meson-loop contributions is modified. In the physical theory of QCD, meson-loop diagrams can be described by two topologically differing types. A typical meson-loop diagram may be decomposed into those where the loop meson contains a sea quark, such as Fig. 1(a), and those where the loop meson is comprised of pure valence quarks, see Fig. 1(b). These diagrams involving the sea quark, type (a), are obviously absent in the quenched approximation and consequently only

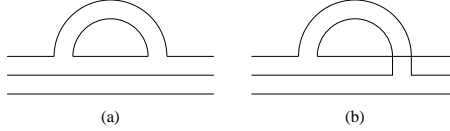


Figure 1. Quark flow diagrams of pion loop contributions appearing in QCD.

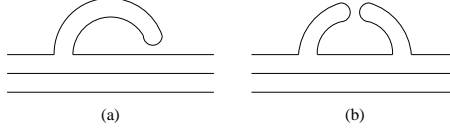


Figure 2. Quark flow diagrams of chiral η' loop contributions appearing in QQCD: (a) axial hairpin, (b) double hairpin.

a subset of the contributions to the physical theory are included. This type of argument, together with SU(6) symmetry, is precisely that described for the evaluation of non-analytic contributions to baryon magnetic moments by Leinweber⁶. This quark flow approach is analogous to the original approach to chiral perturbation theory for mesons performed by Sharpe^{7,8}.

In addition to the usual pion loop contributions, quenched QCD (QQCD) contains loop diagrams involving the flavour singlet η' which also give rise to important non-analytic structure. Within full QCD such loops do not play a role in the chiral expansion because the η' remains massive in the chiral limit. On the other hand, in the quenched approximation the η' is also a Goldstone boson⁸ and the η' propagator has the same kinematic structure as that of the pion.

As a consequence there are two new chiral loop contributions unique to the quenched theory. The first of these corresponds to an axial hairpin diagram such as that indicated in Fig. 2(a). This diagram gives a contribution to the chiral expansion of baryon masses which is non-analytic at order m_π^3 . The second of these new η' loop diagrams arises from the double hairpin vertex as pictured in Fig. 2(b). This contribution is particularly interesting because it involves two Goldstone boson propagators and is therefore the source of more singular non-analytic behaviour – linear in m_π . In studying the extrapolation of quenched lattice results it is essential to treat these contributions on an equal footing to the pion-loop diagrams discussed earlier.

3. Chiral Extrapolations

In general, the coefficients of the leading (LNA) and next-to leading non-analytic (NLNA) terms in a chiral expansion of baryon masses are very large. For instance, the LNA term for the nucleon mass is $\delta m_N^{(\text{LNA})} = -5.6 m_\pi^3$ (with m_π and $\delta m_N^{(\text{LNA})}$ in GeV). With $m_\pi = 0.5$ GeV, quite a low mass for current simulations, this yields $\delta m_N^{(\text{LNA})} = 0.7$ GeV — a huge contribution. Furthermore, in this region hadron masses in both full and quenched lattice QCD are found to be essentially linear in m_π^2 or equivalently quark mass, whereas $\delta m_N^{(\text{LNA})}$ is highly non-linear. The challenge is therefore to ensure the appropriate LNA and NLNA behaviour, *with the correct coefficients*, as $m_\pi \rightarrow 0$, while making a sufficiently rapid transition to the linear behaviour of actual lattice data, where m_π becomes large.

A reliable method for achieving all this was proposed by Leinweber *et al.*⁹ They fit the full (unquenched) lattice data with the form:

$$M_B = \alpha_B + \beta_B m_\pi^2 + \Sigma_B(m_\pi, \Lambda), \quad (1)$$

where Σ_B is the total contribution from those pion loops which give rise to the LNA and NLNA terms in the self-energy of the baryon. The extension to the case of quenched QCD is achieved by replacing the self-energies, Σ_B , of the physical theory by the corresponding contributions of the quenched theory², $\tilde{\Sigma}_B$.

The linear term of Eq. (1), which dominates for $m_\pi \gg \Lambda$, models the quark mass dependence of the pion-cloud source — the baryon without its pion dressing. This term also serves to account for loop diagrams involving heavier mesons, which have much slower variation with quark mass.

The diagrams for the various meson-loop contributions are evaluated using a phenomenological regulator. This regulator has the effect of suppressing the contributions as soon as the pion mass becomes large. At light quark masses the self-energies, Σ_B , provide the same non-analytic behaviour as χ PT, independent of the choice of regulator. Therefore the functional form, Eq. (1), naturally encapsulates both the light quark limit of χ PT and the heavy quark behaviour observed on the lattice.

We consider the leading order diagrams containing only the lightest Goldstone degrees of freedom. These are responsible for the most rapid non-linear variation as the quark mass is pushed down toward the chiral limit. In the physical theory we consider only those diagrams containing pions, as depicted in Fig. 3. In QQCD there exist modified pion loop contributions and the additional structures arising from the η' behaving as a Goldstone boson. The diagrams contributing to the nucleon self-energy in the quenched approximation are shown in Fig. 4, the Δ can be described by analogous diagrams.

$$\Sigma_N = \text{Diagram A} + \text{Diagram B}$$

$$\Sigma_\Delta = \text{Diagram C} + \text{Diagram D}$$

Figure 3. Illustrative view of the meson-loop self-energies, Σ_B , in full QCD. These diagrams give rise to the LNA and NLNA contributions in the chiral expansion. Single (double) lines denote propagation of a N (Δ).

$$\tilde{\Sigma}_N = \begin{array}{c} \text{Diagram 1: } \text{A horizontal line with a dashed semi-circle above it.} \\ + \\ \text{Diagram 2: } \text{A horizontal line with a dashed semi-circle above it.} \\ + \\ \text{Diagram 3: } \text{A horizontal line with a dashed semi-circle above it, with an 'x' at the right end.} \\ + \\ \text{Diagram 4: } \text{A horizontal line with a dashed semi-circle above it, with an 'x' at the right end.} \end{array}$$

Figure 4. Illustrative view of the meson-loop self-energies, Σ_B , in quenched QCD. These diagrams give rise to the LNA and NLNA contributions in the chiral expansion. A cross represents a hairpin vertex in the η' propagator. Single (double) lines denote propagation of a N (Δ).

For the evaluation of the quenched quantities we assume that the parameters of the chiral Lagrangian exhibit negligible differences between quenched and 3-flavour dynamical simulations. This is a working hypothesis with no better guidance yet available, but the successful results of this work demonstrate the self-consistency of such an assumption¹. Only with further accurate lattice simulations at light masses will one be able to determine the extent to which our hypothesis holds.

To highlight the differences in the self-energy contributions we show the net contributions to the Δ in full (Σ_Δ) and quenched ($\tilde{\Sigma}_\Delta$) QCD in Fig. 5. For details of the breakdown of the individual contributions we refer the reader to our longer article². The significant point to note is that whereas the meson cloud of the Δ is attractive in full QCD, it exhibits repulsive behaviour within the quenched approximation.

4. Fitting Lattice Data

The lattice data considered in this analysis comes from the recent paper of Bernard *et al.*⁵ These simulations were performed using an improved Kogut-Susskind quark action, which shows evidence of good scaling¹⁰. Unlike the standard Wilson fermion action, masses determined at finite lattice spacing

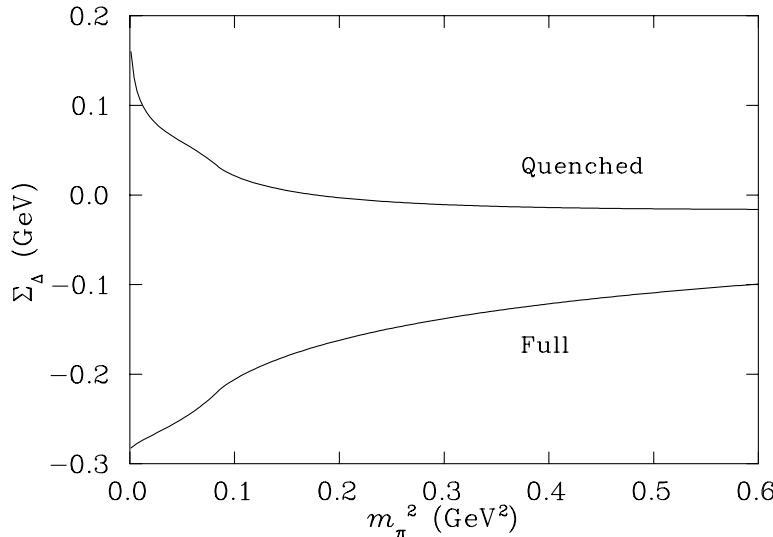


Figure 5. Net contributions to the Δ self-energy evaluated with dipole regulator at $\Lambda = 0.8$ GeV.

are good estimates of the continuum limit results.

We are particularly concerned with the chiral extrapolation of baryon masses and how their behaviour is affected by the quenched approximation. In such a study, it is essential that the method of scale determination is free from chiral contamination. One such method involves the static-quark potential. As low-lying pseudoscalar mesons made of light quarks exhibit negligible coupling to hadrons containing only heavy valence quarks, the low energy effective field theory plays no role in the determination of the scale for these systems. In fixing the scale through such a procedure one constrains all simulations, quenched, 2-flavour, 3-flavour *etc.*, to match phenomenological static-quark forces. Effectively, the short range ($0.35 \sim 0.5$ fm) interactions are matched across all simulations.

A commonly adopted method involving the static-quark potential is the Sommer scale^{11,12}. This procedure defines the force, $F(r)$, between heavy quarks at a particular length scale, namely $r_0 \simeq 0.5$ fm. Choosing a narrow window to study the potential avoids complications arising in dynamical simulations where screening and ultimately string breaking is encountered at large separations. The lattice data analysed in this report uses a variant of this definition, choosing to define the force⁵ at $r_1 = 0.35$ fm via $r_1^2 F(r_1) = 1.00$.

The non-analytic chiral behaviour is governed by the infrared regions of the self-energy integrals. Due to the finite volume of lattice simulations much of

Table 1. Best fit parameters for both full and quenched data sets with dipole regulator, $\Lambda = 0.8$ GeV. All masses are in GeV.

Simulation	α_N	β_N	α_Δ	β_Δ
Physical	1.27(2)	0.90(5)	1.45(3)	0.74(8)
Quenched	1.24(2)	0.85(6)	1.45(4)	0.72(11)

this structure will not be captured. For this reason we evaluate the self-energy corrections with pion momenta restricted to those available on the particular lattice^{2,13}. In this way we get a first estimate of the discretisation errors in the meson-loop corrections. In no way does this account for any artefacts associated with the pion-cloud source.

Current lattice data is insufficient to reliably extract the dipole regulator parameter, Λ . We fit all data choosing a common value to describe all vertices, $\Lambda = 0.8$ GeV. This choice has been optimised² to highlight the main result of this analysis. We note that the value of Λ which we find is indeed consistent with phenomenological estimates which suggest that this should be somewhat less than 1 GeV.

We fit both quenched and dynamical simulation results to the form of Eq. (1) with appropriate discretised self-energies. These fits are shown in Fig. 6. It is the open squares which should be compared with the lattice data. These points correspond to evaluation of the self-energies on the discretised momentum grid. The lines represent a restoration of the continuum limit in the self-energy evaluation. Discrepancies between the continuum and discrete version only become apparent at light quark masses, this corresponds to the Compton wavelength of the pion becoming comparable to the finite spatial extent of the lattice.

The important result of this study is that the behaviour of the pion-cloud source is found to be quite similar in both quenched and dynamical simulations. Once the self-energies corresponding to the given theory are incorporated into the fit, the linear terms are found to be in excellent agreement. Our best fit parameters, for the selected dipole mass $\Lambda = 0.8$ GeV, are shown in Table 1. Here we observe the remarkable agreement between quenched and dynamical data sets for N and Δ masses over a wide range of pion mass. This leads to the interpretation that the primary effects of quenching can be described by the modified chiral structures which give rise to the LNA and NLNA behaviour of the respective theories.

The success of fitting the N and Δ data sets with a common regulator lends confidence to an interpretation of the mass splitting between these states. Examination of the self-energy contributions in full QCD suggests that only about 50 MeV of the observed 300 MeV N - Δ splitting arises from pion loops².

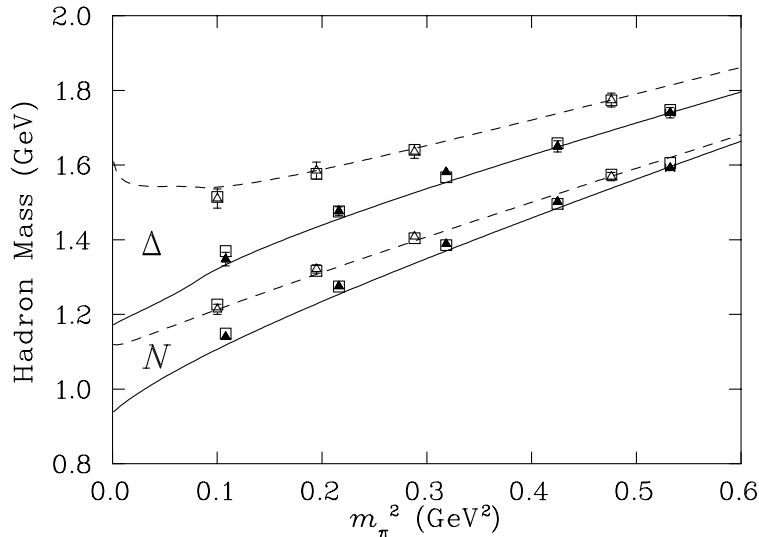


Figure 6. Fit (open squares) to lattice data⁵ (Quenched Δ , Dynamical Δ) with adjusted self-energy expressions accounting for finite volume and lattice spacing artifacts. The infinite-volume, continuum limit of quenched (dashed lines) and dynamical (solid lines) are shown. The lower curves and data points are for the nucleon and the upper ones for the Δ .

The dominant contribution to the hyperfine splitting would then naturally be described by some short-range quark-gluon interactions.

5. Conclusions

We have demonstrated the strength of fitting lattice data with a functional form which naturally interpolates between the domains of heavy and light quarks. The extrapolation formula gives a reliable method for the extraction of baryon masses at realistic quark masses. Although the quenched approximation gives rise to more singular behaviour in the chiral limit, these contributions are quickly suppressed with increasing pion mass. Within the quenched approximation only limited curvature is observed for the N down to low quark masses. In contrast, we find some upward curvature of the Δ mass in the light quark domain.

The observation that the source of the meson cloud has remarkably similar behaviour within both quenched and physical simulations is of considerable importance. One can describe the primary effects of quenching by the meson-loop contributions which give rise to the most rapid, non-linear variation at light quark masses. This leads one to the possibility of applying this result to obtain more physical results from quenched simulations. The structure of

the meson-cloud source can be determined from quenched simulations and then the chiral structures of the physical theory can be incorporated phenomenologically. Natural extension of this work leads to the analysis of further hyperons to investigate the applicability over a range of particles.

References

1. R. D. Young, D. B. Leinweber, A. W. Thomas and S. V. Wright, hep-lat/0111041.
2. R. D. Young, D. B. Leinweber, A. W. Thomas and S. V. Wright, hep-lat/0205017.
3. W. Detmold, D. B. Leinweber, W. Melnitchouk, A. W. Thomas and S. V. Wright, *Pramana* **57**, 251 (2001); nucl-th/0104043.
4. S. Aoki *et al.*, CP-PACS Collaboration, *Phys. Rev. Lett.* **84**, 238 (2000).
5. C. W. Bernard *et al.*, *Phys. Rev.* **D64**, 054506 (2001).
6. D. B. Leinweber, *Nucl. Phys. Proc. Suppl.* **109**, 45 (2002).
7. S. R. Sharpe, *Phys. Rev.* **D41**, 3233 (1990).
8. S. R. Sharpe, *Phys. Rev.* **D46**, 3146 (1992).
9. D. B. Leinweber, A. W. Thomas, K. Tsushima and S. V. Wright, *Phys. Rev.* **D61**, 074502 (2000).
10. C. W. Bernard *et al.*, MILC Collaboration, *Phys. Rev.* **D61**, 111502 (2000).
11. R. Sommer, *Nucl. Phys.* **B411**, 839 (1994).
12. R. G. Edwards, U. M. Heller and T. R. Klassen, *Nucl. Phys.* **B517**, 377 (1998).
13. D. B. Leinweber, A. W. Thomas, K. Tsushima and S. V. Wright, *Phys. Rev.* **D64**, 094502 (2001).